

Photocatalytic Degradation of the Azo Dye “Congo-Red” by $ZnFe_2O_4/ZnO$ Nanocomposite

Zulfiqar Ahmed Mohammed Nazeer^{1*}, M. Praveen², R. Harikrishna³, Mohan Kumar⁴,
Shobha Nagarajaiah⁵ and B. M Nagabhushana³

¹Engineering Department, University of Technology and Applied Sciences – Ibri, Ibri - 516, Sultanate of Oman; zulfi_chem@yahoo.com

²Centre for Advanced Materials Technology (CAMT), RIT, Bengaluru – 560054, Karnataka, India; saintypraveen@gmail.com

³Department of Chemistry, M. S. Ramaiah Institute of Technology, Bengaluru - 560054, Karnataka, India

⁴Department of Chemistry, PES Institute of Technology, Shivamogga –577204, Karnataka, India

⁵Department of Chemistry, Maharani Science College for Women, Bengaluru – 560054, Karnataka India

Abstract

This paper reports the preparation of $ZnFe_2O_4/ZnO$ metal oxide nanocomposite by solution combustion synthesis. Zinc nitrate and ferric nitrate were utilized as oxidizers in this work, while glycine served as fuel. The powder X-ray diffraction pattern indicated that the nanocomposite consisted of $ZnFe_2O_4$ and ZnO having spinel and wurtzite phases respectively. The efficiency of the nanocomposite in the photocatalytic degradation of Congo Red (CR) dye from its aqueous solution was studied. The effects of CR starting concentration, photocatalyst dose, and irradiation duration were investigated. More than 90 % degradation of 10 ppm CR solution was achieved for a photocatalyst dosage of 1.0g/litre of the dye solution in 40 minutes. The excellent photocatalytic activity of the nanocomposite was considered as the result of the synergistic mechanism between its constituent phases, significantly reducing electron-hole recombination. It was noticed that the photocatalyst after the first regeneration was about 85 % efficient compared to the original one. The water contamination with human activity can be reduced by the usage of $ZnFe_2O_4/ZnO$ metal oxide nanoparticles.

Keywords: Congo Red, Nanocomposite, Synergistic Mechanism, $ZnFe_2O_4/ZnO$ Metal Oxide

1.0 Introduction

Treating polluted water contaminated by human activity will be a challenging task in the future¹. Azo dyes contain the azo ($-N=N-$) chromophores and constitute one of the significant classes of dyes used in textile and other industries². Azo dyes such as Congo Red (CR) and their degradation products such as aromatic amines exhibit carcinogenic effects when present in wastewater³.

Hence, it is of prime importance to treat the effluents containing such dyes to minimize their effect on the environment⁴.

Some commonly used methods for removing dyes from wastewater include adsorption, biodegradation, chlorination, ozonation, flocculation, reverse osmosis, etc. Most of these methods are not destructive since they only transfer the contaminant from one phase into the other, requiring further treatment⁵.

*Author for correspondence

Recently, advanced oxidation processes, commonly called AOPs, are being considered as one of the most effective methods for removing toxic and non-biodegradable pollutants from wastewater⁶. Photocatalysis, H₂O₂/UV, and the Fenton process are the commonly used AOPs. AOPs generate hydroxyl radicals (●OH) which are potent oxidizing species responsible for the mineralization of organic matter into H₂O and CO₂⁷.

Heterogeneous photocatalysis using metal oxide nanomaterials is considered to be less expensive and more efficient method for removing various pollutants from wastewater. This process involves the oxidation of pollutants on the surface of the photocatalyst. This method results in quick oxidation of the pollutants and does not form polycyclic compounds⁸. The process can efficiently remove inorganic and organic pollutants and microbes from water. However, a significant drawback of this process is the quick recombination of the photogenerated electrons and holes, which decreases the efficiency of the photocatalyst⁹.

Semiconductor metal oxide nanoparticle combination is one of the promising techniques to minimize charge recombination. The formation of nanocomposite is an important feature of this technique. A wide band gap semiconductor is coupled with a narrow band gap semiconductor in the nanocomposite material. These two semiconductors should possess matching band potentials. When such a nanocomposite photocatalyst is illuminated with UV or visible light, there is the generation of electrons and holes in the narrow band gap semiconductor, which initiates the photocatalytic reaction, thus increasing the photocatalytic efficiency⁹. Recently, several nanocomposite photocatalysts have been prepared, and their photocatalytic efficiencies in the degradation of dyes have been reported. Some of these include metal oxide composites such as MgFe₂O₄/TiO₂, NiFe₂O₄/TiO₂, CuFe₂O₄/TiO₂, MnFe₂O₄/TiO₂ and ZnFe₂O₄/TiO₂¹⁰. TiO₂/AgGaS₂ photocatalyst was synthesized by sol-gel synthesis and solid-state reaction¹¹. The photocatalyst exhibited excellent photocatalytic activity in comparison to its constituents. The higher charge separation and quick photogenerated electron transport from AgGaS₂ to TiO₂ were credited with this exceptional photocatalytic activity.

The co-precipitation method was employed to successfully synthesize nanocrystalline Fe-Ce mixed

metal oxides¹². The mixed oxide almost completes the degradation of CR from its aqueous solution. This was attributed to the mixed oxide's greater surface area and surface acidity¹³.

The synthesis of ZnFe₂O₄/ZnO nano composite metal oxide was described in the current work using solution combustion synthesis. Congo Red was successfully removed from its aqueous solution using the nanocomposite. Researchers looked at the effects of photocatalyst dosage, irradiation duration, and starting CR concentration. It was also investigated as to how regeneration affected the photocatalyst's efficiency.

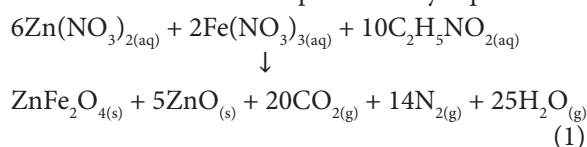
2.0 Materials and Methods

Ferric nitrate [99%, SD Fine Chemicals Ltd., India], Zinc nitrate [99%, SD Fine Chemicals Ltd., India], and Glycine [99%, SD Fine Chemicals Ltd., India] were supplied by SD-Fine Chemicals Limited, India. The chemicals were used as received without further purification.

2.1 Preparation of the ZnFe₂O₄/ZnO Metal Oxide Nanocomposite

Appropriate amounts of ferric nitrate, zinc nitrate, and Glycine were transferred into the reaction vessel and were dissolved in a minimum quantity of double distilled water. The solution was stirred on a magnetic stirrer for ~10 minutes and then heated on a hotplate to evaporate excess water. The reaction vessel was then placed into a muffle furnace at ~350°C. Initially, there was dehydration of the reaction mixture followed by combustion, thus forming the nanocomposite. After allowing the nanocomposite to reach room temperature, it was finely crushed into a powder^{14,15}.

The entire reaction was represented by Equation 1.



2.2 Characterization of the ZnFe₂O₄/ZnO Nanocomposite

The nanocomposite's PXRD data was acquired using the 40 kV CuKα radiation Philips X'Pert Pro X-ray diffractometer. The nanocomposite's average crystallite

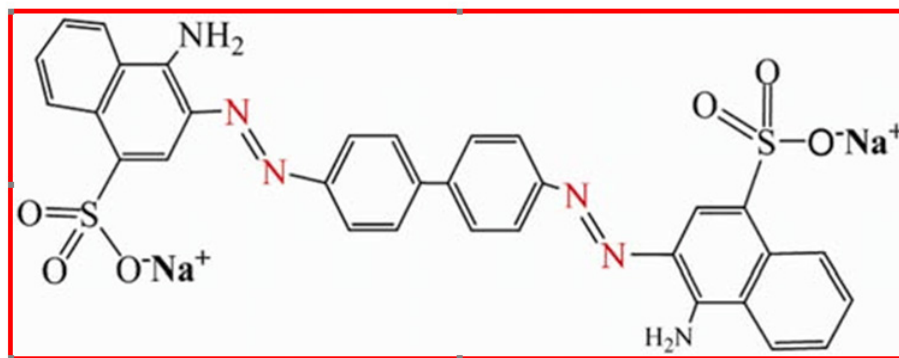


Figure 1. Structure of CongoRed Dye.

size (D) was calculated using Equation 2, also known as Scherer's formula.

$$D = \frac{k\lambda}{\beta \cos\theta} \quad (2)$$

Bragg's angle (θ), the full width at half maximum (β), and the wavelength (λ) of the X-rays were obtained from the XRD pattern and the instrument¹⁶.

Using KBr as a reference, the Perkin-Elmer spectrometer (spectrum 1000) was utilized to record the nanocomposite's FTIR spectrum. The scanning electron micrograph of the nanocomposite was captured using a JEOL-2100F (Japan) scanning electron microscope.

2.3 Photocatalytic Degradation of the Congo Red Dye

The Congo Red is a water-soluble azo dye having the structure shown in Figure 1. In human beings, it affects the eyes, skin, respiratory, and reproductive systems. In higher concentrations, it shows cytotoxic, carcinogenic as well as mutagenic effects. Figure 2 depicts the UV-visible spectrum of CR (10 ppm) which showed maximum absorbance at 498 nm¹⁶.

A suitable quantity of the nanocomposite and 50 millilitres of CR solution were added to the reaction vessel. The liquid was centrifuged for ten minutes after being magnetically agitated for thirty minutes while exposed to UV radiation. Equation 3 was used to compute the percentage of dye removal after the UV-visible spectra of the supernatant solution were recorded¹⁷.

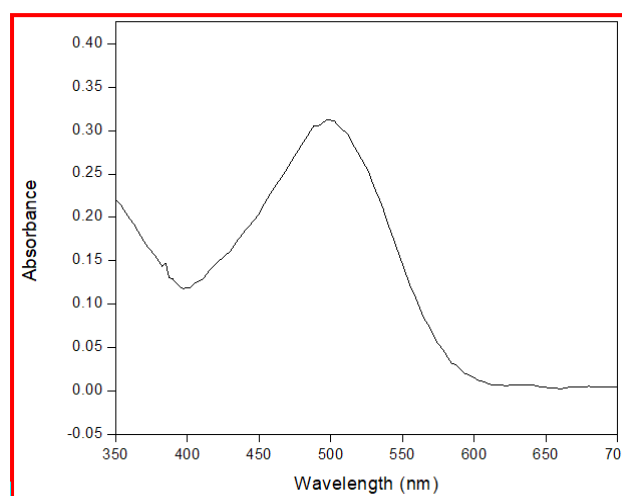


Figure 2. Absorbance of 10 ppm Congo red Dye solution.

$$\% \text{ dye removal} = \frac{(C_0 - C_e)}{C_0} \times 100 \quad (3)$$

C_0 and C_e refer, respectively, to the initial and equilibrium concentrations of the CR solution. The process described above was carried out using different photocatalyst dosages. Figure 6 shows the photocatalyst dosage that works best.

After the ideal dosage was established, 100 mL of CR solution and the ideal quantity of the nanocomposite were added to the reaction vessel to examine the impact of irradiation duration. Under UV light, the slurry was magnetically agitated. A little aliquot of the mixture was taken out and centrifuged every five minutes, and each time the supernatant's UV-visible spectrum was measured. Figure 7 shows the optimal period to be exposed to radiation¹⁸.

2.4 Reusability of the Photocatalyst

Reusability tests were conducted for the ZnFe₂O₄/ZnO nanocomposite. After being used in the photocatalytic degradation experiment, the photocatalyst was allowed to settle down naturally in the reactor. The supernatant dye solution was removed by decantation. The residue was washed several times with double distilled water and then dried for 5 hours at 60 °C before being used for new photocatalytic degradation experiments. The studies were carried out after the first and second regeneration. The reusability studies were conducted for 10 ppm CR solution¹⁹.

3.0 Results and Discussions

3.1 Characterization of the ZnFe₂O₄/ZnO Nanocomposite

3.1.1 XRD Studies

The ZnFe₂O₄-ZnO nanocomposite's PXRD pattern (Figure 3) revealed the existence of the wurtzite phase of ZnO (JCPDS file number: 36-1451) and the spinel phase of ZnFe₂O₄ (JCPDS file number: 22-1012). Equation 2 yielded an average crystallite size of around 15 nm¹⁷.

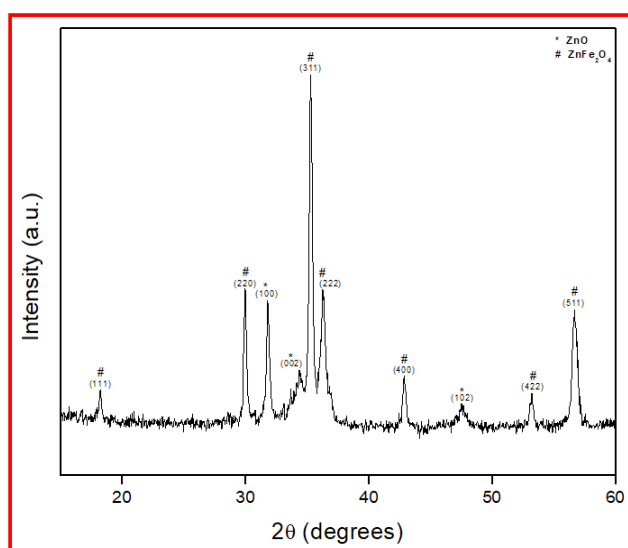


Figure 3. PXRD pattern of the ZnFe₂O₄-ZnO nanocomposite.

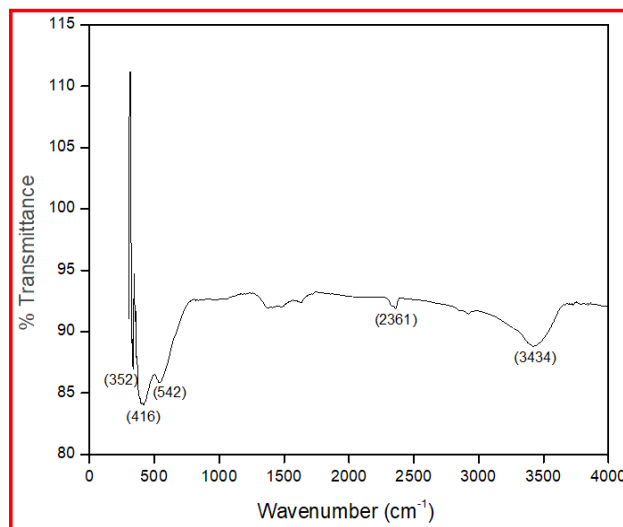


Figure 4. FTIR spectrum of the ZnFe₂O₄-ZnO nanocomposite.

3.1.2 FTIR Studies

The ZnFe₂O₄-ZnO nanocomposite's FTIR spectra (Figure 4) revealed peaks for both the Zn-O (~352 cm⁻¹) and Fe-O (~416 and ~542 cm⁻¹) linkages. The -OH group of water adsorbed on the photocatalyst surface and ambient CO₂ were responsible for the maxima at approximately 2361 cm⁻¹ and 3434 cm⁻¹, respectively²⁰.

3.1.3 SEM Studies

The SEM micrograph of the nanocomposite (Figure 5) showed that the particles were highly agglomerated. The agglomeration was due to the tendency of the particles to minimize their surface-free energy²¹.

3.2 Photocatalytic Degradation Studies

Figures 6 and 7 depict the results of the photocatalytic removal of CR. As the photocatalyst dosage increased, the dye degradation increased until the optimum dosage was reached. The optimum dosage was found to be 1.0 gL⁻¹ for both the initial dye concentrations. Beyond 1.0 gL⁻¹, the dye degradation was negligible. It was discovered that 40 minutes was the ideal irradiation time. The photocatalyst's number of active sites rose along with its dosage, which raised the rate at which CR degraded²².

The photocatalytic degradation of CR decreased with its initial concentration (Table 1). This was because the number of dye molecules increased when the initial CR

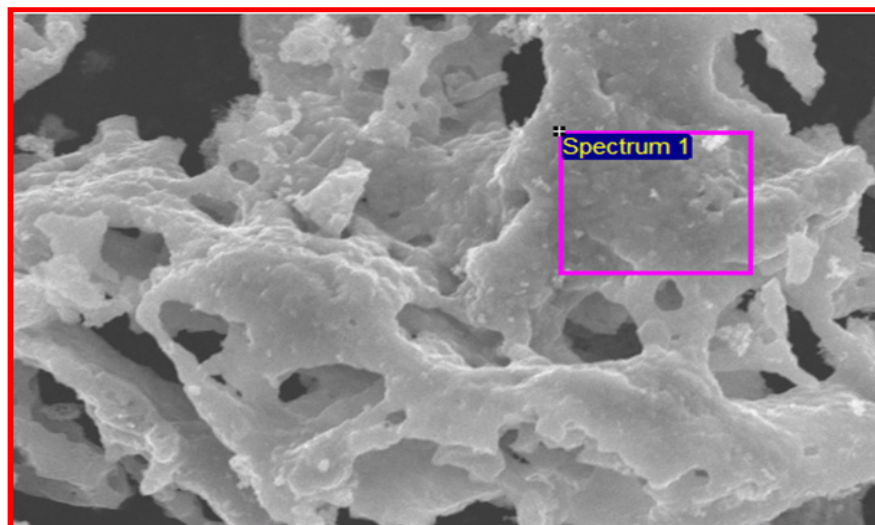


Figure 5. SEM micrograph of the ZnFe₂O₄-ZnO nanocomposite.

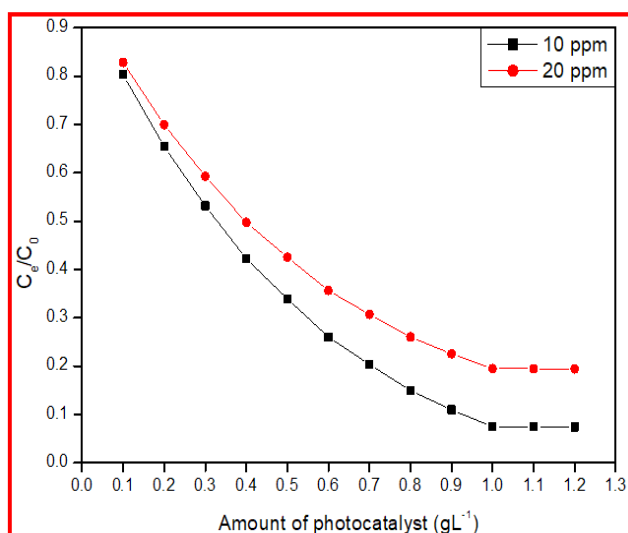


Figure 6. Effect of dosage of the photocatalyst.

concentration was increased for a given dosage of the nanocomposite. Still, the number of active sites remained the same. The competition amongst the dye molecules to adsorb onto the photocatalyst's active sites increased as the initial concentration of the dye increased²².

3.3 Reusability of the Photocatalyst

Table 2 gives the results of the reusability studies. It was found that the efficiency of the photocatalyst decreased with usage (Figure 8). After the first use, the photocatalyst

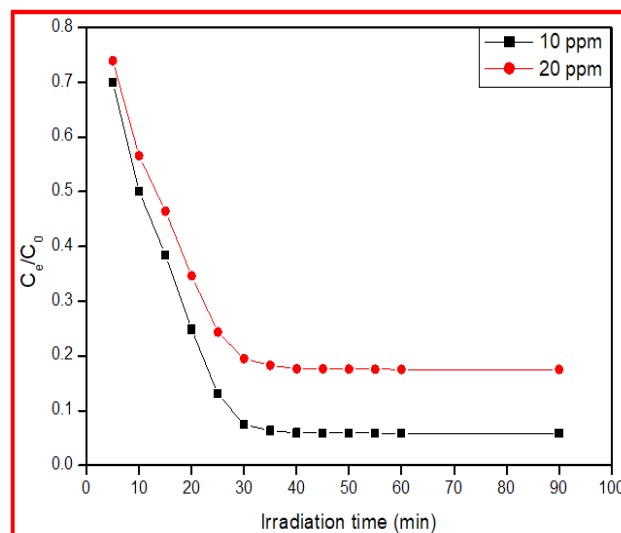


Figure 7. Effect of irradiation time.

was almost 85% more efficient in degrading CR than the original one. The efficiency was further reduced after the first and second usage. Also, there was a slight increase in the dosage of the nanocomposite as well as the irradiation time²³.

3.4 Mechanism of Photocatalytic Degradation of Congo Red

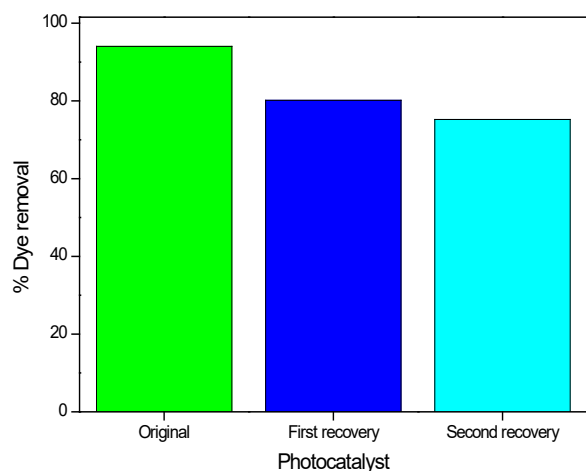
As is evident from the results, the ZnFe₂O₄/ZnO nanocomposite exhibited excellent photocatalytic

Table 1. Results for the photocatalytic degradation of Congo red dye

Concentration of the Dye solution (ppm)	Optimum Dosage of the Photocatalyst (gL^{-1})	Optimum Irradiation Time (min)	% Dye Removal
10	1.0	40	94.03
20	1.0	40	82.34

Table 2. Reusability of the photocatalyst after first and second recovery

Nature of the photocatalyst	Optimum Dosage of the Photocatalyst (gL^{-1})	Optimum Irradiation Time (min)	% Dye Removal
Original	1.0	40	94.03
First recovery	1.1	45	80.15
Second recovery	1.2	50	75.22

**Figure 8.** Results of reusability of the photocatalyst.

activity for the removal of CR from its aqueous solution. This was attributed to the presence of both ZnFe_2O_4 and ZnO phases, resulting in a synergistic mechanism between them. The synergistic mechanism

involved interparticle charge transfer from one phase to another²⁴.

The $\text{ZnFe}_2\text{O}_4/\text{ZnO}$ nanocomposite's photocatalytic degradation mechanism can be explained in the following way. When the nanocomposite is exposed to UV radiation, the semiconductors ZnFe_2O_4 and ZnO within it are excited, which causes electron-hole pairs to form in each semiconductor. Every semiconductor has stimulated electrons that move from its Valence Band (VB) to its matching Conduction Band (CB). The CB of ZnFe_2O_4 contains electrons that leap into that of ZnO 's, boosting the latter's electron concentration²⁵.

The holes in ZnO 's VB shift to that of ZnFe_2O_4 at the same time. As a result, there are more holes in the ZnFe_2O_4 VB. More charge separation and a notable decrease in electron-hole recombination are the outcomes of this process. The redox processes that take place at the semiconductor surfaces involve both electrons and holes. Overall, this leads to a rise in photocatalytic activity. The improved electron-hole charge separation in the nanocomposite was the cause of its increased photocatalytic activity²⁶.

4.0 Conclusions

ZnFe₂O₄-ZnO nanocomposite was prepared for this study using the solution combustion method. The product was characterised using FTIR, SEM, and PXRD. Excellent photocatalytic effectiveness was demonstrated by the nanocomposite in the extraction of CR from its aqueous solution. As a result, the ZnFe₂O₄-ZnO nanocomposite shows promise as a photocatalyst for the efficient extraction of colours from wastewater. So the material we have studied in this work will be a promising combination for effective dye removal from the industrial effluent water.

5.0 Acknowledgement

The M.S. Ramaiah Institute of Technology, Bengaluru's Chemistry Department, and the Centre for Advanced Materials Technology (CAMT), M.S. Ramaiah Institute of Technology are acknowledged by the authors for their assistance.

6.0 References

- Santhosh AM, Yogendra K, Madhusudhana N, Mahadevan KM, Veena SR. Efficient photodegradation of Victoria Blue B and Acridine Orange dyes by nickel oxide nanoparticles. *Mater Today Proc.* 2023; 92(Part 2): 1616-22. <https://doi.org/10.1016/j.matpr.2023.06.089>
- Lang W, Sirisansaneeyakul S, Tagami T, Kang H-J, Okuyama M, Sakairi N, *et al.* Nonreducing terminal chimeric isomaltomegalosaccharide and its integration with azoreductase for the remediation of soil-contaminated lipophilic azo dyes. *Carbohydr Polym.* 2023; 305. <https://doi.org/10.1016/j.carbpol.2023.120565> PMID:36737177
- Sharma B, Tiwari S, Kumar R, Kumar M, Tewari L. Eco-friendly detoxification of hazardous Congo red dye using novel fungal strain *Trametes flavida* WTFP2: Deduced enzymatic biomineralization process through combinatorial in-silico and in-vitro studies. *J Hazard Mater.* 2023; 455. <https://doi.org/10.1016/j.jhazmat.2023.131503> PMID:37150098
- Pandian SA, Sivakumar M. Barium titanate perovskite nanoparticles integrated reduced graphene oxide nanocomposite photoanode for high performance dye-sensitized solar cell. *Results Chem.* 2023; 6. <https://doi.org/10.1016/j.rechem.2023.101091>
- Nachiyar CV, Rakshi AD, Sandhya S, Jebasta NBD, Nellore J. Developments in treatment technologies of dye-containing effluent: A review. *Case Stud Chem Environ Eng.* 2023; 7. <https://doi.org/10.1016/j.cscee.2023.100339>
- Mahadevi P, Sumathi S. Schiff base metal complexes: Synthesis, optoelectronic, biological studies, fabrication of zinc oxide nanoparticles and its photocatalytic activity. *Results Chem.* 2023; 6. <https://doi.org/10.1016/j.rechem.2023.101026>
- Jiang H, Sathiyavimal S, Cai L, Devanesan S, Sayed SRM, Jhanani GK, *et al.* Tulsi (*Ocimum sanctum*) mediated Co nanoparticles with their anti-inflammatory, anti-cancer, and methyl orange dye adsorption properties. *Environ Res.* 2023; 236. <https://doi.org/10.1016/j.envres.2023.116749> PMID:37507040
- Kumari P, Kumar A. Advanced oxidation process: A remediation technique for organic and non-biodegradable pollutant. *Results in Surfaces and Interfaces.* 2023; 11. <https://doi.org/10.1016/j.rsufi.2023.100122>
- Zhou L, Li B, Li J, Wang S, Huang H, Lu C, *et al.* Simultaneous triple-effect on inhibiting the photogenerated carriers recombination of g-C₃N₄ for boosting solar H₂ production at atmospheric pressure. *J Environ Chem Eng.* 2023; 11(3). <https://doi.org/10.1016/j.jece.2023.109975>
- Tejashwini DM, Harini HV, Nagaswarupa HP, Naik R, Deshmukh VV, Basavaraju N. An in-depth exploration of eco-friendly synthesis methods for metal oxide nanoparticles and their role in photocatalysis for industrial dye degradation. *Chem Phys Impact.* 2023; 7. <https://doi.org/10.1016/j.chphi.2023.100355>
- Obayomi KS, Lau SY, Ibrahim O, Zhang J, Meunier L, Aniobi MM, *et al.* Removal of Congo red dye from aqueous environment by zinc terephthalate metal organic framework decorated on silver nanoparticles-loaded biochar: Mechanistic insights of adsorption. *Microporous Mesoporous Mater.* 2023; 355. <https://doi.org/10.1016/j.micromeso.2023.112568>
- Jiang R-N, Chen Y-A, Liu Y, Liu H. Multi-functional nanocomposite hydrogels based on assembled catechin-modified TiO₂ nanoparticle crosslinker for efficient dye removal from wastewater. *Mater Today Commun.* 2023; 37. <https://doi.org/10.1016/j.mtcomm.2023.107216>
- Vinayagam V, Palani KN, Ganesh S, Rajesh S, Akula VV, Avoodaiappan R, *et al.* Recent developments on advanced oxidation processes for degradation of pol-

- lutants from wastewater with focus on antibiotics and organic dyes. *Environ Res.* 2024; 240. <https://doi.org/10.1016/j.envres.2023.117500> PMID:37914013
14. Praveen M, Karthikeya GS, Krishna RH, Mamatha GM, Manjunatha C, Khosla A, *et al.* The role of magnetic nano CoFe_2O_4 and conductive MWCNT/graphene in LDPE-based composites for electromagnetic interference shielding in X-band. *Diam Relat Mater.* 2022; 130. <https://doi.org/10.1016/j.diamond.2022.109501>
 15. Manjappa P, Rajan HK, Mahesh MG, Sadananda KG, Channegowda M, Shivashankar GK, *et al.* Effective attenuation of electromagnetic waves by synergetic effect of $\alpha\text{-Fe}_2\text{O}_3$ and MWCNT/Graphene in LDPE-based composites for EMI applications. *Materials.* 2022; 15(24). <https://doi.org/10.3390/ma15249006> PMID:36556812 PMCid:PMC9785817
 16. Punnakkal VS, Anila EI. Polypyrrole/silver/graphene ternary nanocomposite synthesis and study on photocatalytic property in degrading Congo red dye under visible light. *Surf Interfaces.* 2023; 42. <https://doi.org/10.1016/j.surfin.2023.103342>
 17. Ibhadon AO, Greenway GM, Yue Y. Photocatalytic activity of surface modified $\text{TiO}_2/\text{RuO}_2/\text{SiO}_2$ nanoparticles for azo-dye degradation. *Catal Commun.* 2008; 9(1):153-7. <https://doi.org/10.1016/j.catcom.2007.05.038>
 18. Nagaraja R, Kottam N, Girija CR, Nagabhushana BM. Photocatalytic degradation of Rhodamine B dye under UV/solar light using ZnO nanopowder synthesized by solution combustion route. *Powder Technol.* 2012; 215-216:91-7. <https://doi.org/10.1016/j.powtec.2011.09.014>
 19. Bhagya NP, Prashanth PA, Raveendra RS, Sathyanarayani S, Ananda S, Nagabhushana BM, *et al.* Adsorption of hazardous cationic dye onto the combustion derived SrTiO_3 nanoparticles: Kinetic and isotherm studies. *J Asian Ceram Soc.* 2016; 4(1):68-74. <https://doi.org/10.1016/j.jascr.2015.11.005>
 20. Panda SSS, Gandhi S, Parne SR, Panigrahi T, Parambil VV. Facile hydrothermal synthesis of bio-inspired $\text{ZnO}/\text{Fe}_2\text{O}_3/\text{ZnFe}_2\text{O}_4$ heterostructure: Effect of microwave absorption properties. *Surf Interfaces.* 2023; 42. <https://doi.org/10.1016/j.surfin.2023.103490>
 21. Lin K, Zhao Y, Kuo J-H, Lin C-L. Agglomeration-influenced transformation of heavy metals in gas-solid phases during simulated sewage sludge co-incineration: Effects of phosphorus and operating temperature. *Sci Total Environ.* 2023; 858. <https://doi.org/10.1016/j.scitotenv.2022.159759> PMID:36349628
 22. Chaibeddra D, Benamira M, Colmont M, Boulehbali H, Lahmar H, Avramova I, *et al.* Synthesis, physical and electrochemical characterization of CoCr_2O_4 and its application as photocatalyst under solar irradiation. *Inorganic Chem Comm.* 2023; 155. <https://doi.org/10.1016/j.inoche.2023.111116>
 23. Adarsha JR, Ravishankar TN, Manjunatha CR, Ramakrishnappa T. Green synthesis of nanostructured calcium ferrite particles and its application to photocatalytic degradation of Evans blue dye. *Mater Today Proc.* 2022; 49:777-88. <https://doi.org/10.1016/j.matpr.2021.05.293>
 24. Sakkas VA, Islam MA, Stalikas C, Albanis TA. Photocatalytic degradation using design of experiments: A review and example of the Congo red degradation. *J Hazard Mater.* 2010; 175(1):33-44. <https://doi.org/10.1016/j.jhazmat.2009.10.050> PMID:19931983
 25. Vergis BR, Hari Krishna R, Kottam N, Nagabhushana BM, Sharath R, Darukaprasad B. Removal of malachite green from aqueous solution by magnetic CuFe_2O_4 nano-adsorbent synthesized by one pot solution combustion method. *J Nanostructure Chem.* 2018; 8(1):1-12. <https://doi.org/10.1007/s40097-017-0249-y>
 26. Das S, Paul SR, Debnath A. Methyl red dye abatement from aqueous solution using calcium ferrite and manganese ferrite magnetic nanocomposite: Kinetics and isotherm study. *International Conference on Multidimensional Sustainability: Advanced Technologies for Industrial Pollution Control ATIPC 2022: Sustainable Advanced Technologies for Industrial Pollution Control*; 2023. p. 13-26. https://doi.org/10.1007/978-3-031-37596-5_2